IEEE Photonics Journal
An IEEE Photonics Society Publication

Open Access

Optimized Support Vector Machine Assisted BOTDA for Temperature Extraction With Accuracy Enhancement

Volume 12, Number 1, February 2020

Hongna Zhu
Lei Yu
Yufeng Zhang
Le Cheng
Zhenyu Zhu
Jiayin Song
Jinli Zhang
Bin Luo
Kai Yang

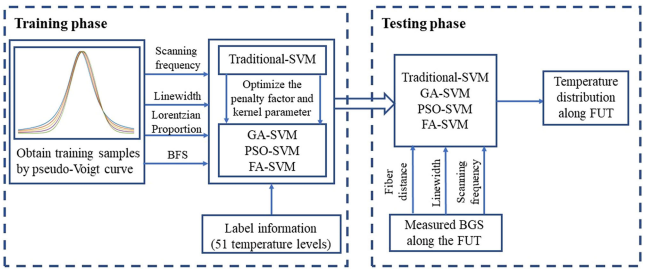

DOI: 10.1109/JPHOT.2019.2957410

Optimized Support Vector Machine Assisted BOTDA for Temperature Extraction With Accuracy Enhancement

Hongna Zhu,[1] Lei Yu,[1] Yufeng Zhang,[1] Le Cheng,[1] Zhenyu Zhu,[1] Jiayin Song,[1] Jinli Zhang,[2] Bin Luo,[3] and Kai Yang [1]

[1]School of Physical Science and Technology, Southwest Jiaotong University, Chengdu 610031, China
[2]National Key Laboratory of Science and Technology on Blind Signal Processing, Chengdu 610041, China
[3]School of Information Science and Technology, Southwest Jiaotong University, Chengdu 610031, China

DOI:10.1109/JPHOT.2019.2957410

Manuscript received October 22, 2019; revised November 25, 2019; accepted November 30, 2019. Date of publication December 3, 2019; date of current version January 7, 2020. This work was supported in part by the National Natural Science Foundation of China under Grant 61405167 and in part by the Fundamental Research Funds for the Central Universities under Grants 2682018GF10 and 2682019LK08. Corresponding author: Kai Yang (e-mail: yangkai_swjtu@163.com).

Abstract: Brillouin optical time domain analyzer (BOTDA) assisted by optimized support vector machine (SVM) algorithm for accurate temperature extraction is presented and experimentally demonstrated. Three typical intelligent optimization algorithms, particle swarm optimization algorithm, genetic algorithm and firefly algorithm are explored to optimize the SVM parameters. The performances of optimized SVM algorithms for temperature extraction are investigated in both simulation and experiment under different conditions for Brillouin gain spectrum collection, resulting in the significant enhancement of sensing accuracy. In particular, the extraction accuracy (i.e., smaller root mean square error value) of temperature information is improved about 4 °C compared with the conventional SVM when the signal-to-noise ratio (SNR) as low as 2.5 dB and 40-ns pump pulse width are adopted in the experiment. In addition to the enhanced accuracy with good robustness, the optimized algorithms have faster processing speed than the curve fitting method, over 20-times improvement. That makes the optimized algorithms become a very promising candidate for high performance BOTDA sensors in the future.

Index Terms: Brillouin optical time domain analyzer, fiber optics sensors, support vector machine, optimized algorithms.

1. Introduction

With multiple advantages of high spatial resolution, large dynamic range and real-time monitoring, distributed optical fiber sensor has attracted great attentions and it has been intensively researched and widely used in various fields [1]–[4]. Among the numerous distributed optical fiber sensors, Brillouin optical time domain analyzer (BOTDA) is a typical distributed optical fiber sensor and has attracted increasing research attentions due to its characteristics of precise temperature and strain monitoring along ultra-long sensing range [5]–[7].

In order to extract the temperature and strain information in a BOTDA system, the Brillouin frequency shift (BFS) should be estimated from the measured Brillouin gain spectrum (BGS).

Generally, the curve fitting methods are utilized to extract the BFS and the frequency of peak gain on fitted curve is taken as the BFS. In BOTDA, Lorentzian Curve Fitting (LCF) [8]–[10], Gaussian curve [11] and pseudo-Voigt curve fitting (pVCF) [12], [13] have been adopted. To avoid the complex initial parameters setting in the fitting process, a cross-correlation method (XCM) is proposed to extract the BFS [14]. However, it takes more executing time to obtain the same accuracy in comparison with LCF algorithm. Besides, the artificial neural network (ANN) is introduced into the BOTDA system to realize high-accuracy and real-time monitoring. But, the complicated training process, large time consumption and frequent updates of the ANN architecture restrict its practicability [15], [16].

In order to extract the BFS efficiently, support vector machine (SVM) has been successfully employed in BOTDA. SVM is a popular signal processing method and it has been widely used in data classification and regression owing to its outstanding capability and small computation cost [17]–[19]. Compared with the neural network, SVM has faster learning convergence, shorter time consuming and less storage requirements for ultrafast temperature extraction in BOTDA [20]–[22]. More importantly, SVM algorithm achieves comparative demodulation accuracy compared to the curve-fitting methods. However, the accuracy of BOTDA based on SVM should be improved further especially at low SNR range for some practical applications.

In this paper, optimized algorithms are utilized to modify the operation parameters of SVM for accuracy improvement of the temperature extraction in SVM assisted BOTDA. Three types of SVM classifiers including particle swarm optimization algorithm (PSO) [23], genetic algorithm (GA) [24] and firefly algorithm (FA) [25] are adopted to optimize the SVM. The improvement of the demodulation accuracy with the three optimization algorithms have been carefully analyzed. The tolerance of optimized SVM algorithms to different pump pulse widths, frequency scanning steps and SNRs are investigated both in the simulation and experiment. The verification tests are in good agreement with the simulation. Compared with conventional SVM, all optimized SVM algorithms improve the measurement accuracy greatly and the maximum enhancement is about 4 °C. Although the processing time increases slightly by adopting the optimization, it is acceptable by considering the significant improvement of accuracy. Especially, the processing speed improves over 20 times in comparison with the curve fitting method.

2. Principle and Simulations

2.1 Principle of the Adopted SVM

SVM is a supervised learning algorithm which is used to solve binary classification problem. Through a feature mapping ϕ, the training data is mapped to high dimensional characteristic space F and linear regression is carried out in this space. For a training sample of $D = ((x_1, y_1), (x_2, y_2), \ldots, (x_i, y_i), \ldots, (x_n, y_n))$, the feature space F is divided by a hyperplane and the hyperplane is expressed by

$$y = \langle w, \phi(x) \rangle + b \tag{1}$$

where $w = (w_1, w_2, \ldots, w_d)$ is the normal vector and it determines the direction of the hyperplane. b is a displacement and it determines the distance ($b/||w||$) between the hyperplane and the coordinate origin, as shown in Fig. 1. The interval $\gamma = 1/||w||$ is determined by the minimum distance between the raw data and the hyperplane. To distinguish different categories exactly, γ must be maximized under the condition of $y_i(w^t x_i + b) \geq 1$. The optimal hyperplane is acquired with the following constraint function [26]:

$$\begin{aligned} \min_{w,b} \quad & \tfrac{1}{2}||w||^2 \\ \text{s.t.} \quad & y_i(w^T x_i + b) \geq 1 \quad i = 1, 2, \ldots, N \end{aligned} \tag{2}$$

In order to calculate γ, the Lagrangian multipler α_i must be adopted [27]. Besides, the penalty factor C is introduced to deal with the unclassifiable problem and it restricts the range of α_i. On the other hand, it difficult to calculate Eq. (2) owing to the high dimension of the feature space

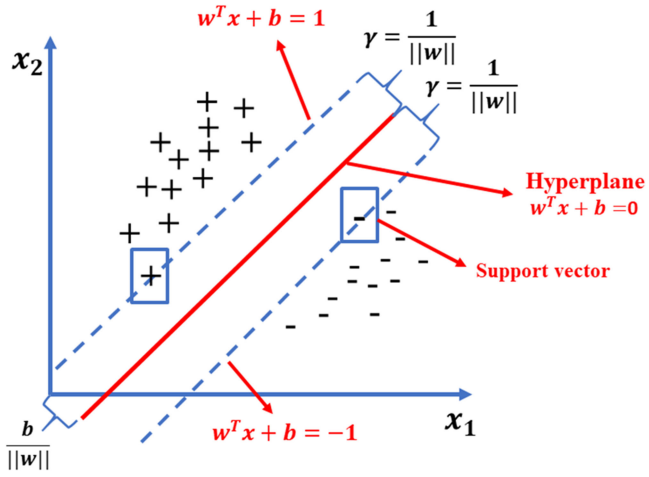

Fig. 1. Support vector and interval.

F. To overcome this problem, the kernel function $K(x_i, x_j) = <\Phi(x_i), \Phi(x_j)>$ is introduced and the linear SVM is transformed into non-linear SVM. With that, the optimization of the hyperplane is transformed into the convex quadratic programming problem and the optimized function is described as

$$\begin{aligned} \min_{\alpha} \quad & \frac{1}{2}\sum_{i=1}^{n}\sum_{j=1}^{n}\alpha_i\alpha_j y_i y_j K(x_i, x_j) - \sum_{i=1}^{n}\alpha_i \\ \text{s.t.} \quad & \sum_{i=1}^{n}\alpha_i y_i = 0 \\ & 0 \le \alpha_i \le C \qquad i = 1, 2, \ldots, n \end{aligned} \tag{3}$$

In Eq. (3), C makes a tradeoff between the interval (γ) and the classification error. With the change of C, the classification error varies accordingly. But unfortunately, there is no definite relation between C and classification error. In our work, a radial basis function (RBF) is utilized as the kernel function $K(x_i, x_j)$, as illustrated in Eq. (4). Note that, the distribution of the data in feature space F is determined by σ.

$$K(x_i, x_j) = \exp\left(-\frac{||x_i - x_j||_2^2}{2\sigma^2}\right) \tag{4}$$

In BOTDA, the temperature extraction is considered as a classification problem and the measured BGSs are divided into the corresponding temperature classes with the multi-class SVM. SVM algorithm consists of training and test phases. In the training phase, the temperature is divided into 51 categories with step of 1 °C. After that, each measured BGS is classified into the corresponding class of temperatures in the test phase. Here, the corresponding temperature value is taken as the measured temperature.

2.2 Principle of Optimization Algorithms

Although linear SVM has been served as an efficient approach for the BFS extraction in BOTDA, its performance needs to be optimized since the parameters of C (penalty factor) and σ (kernel parameter) is not optimal. In previous works, σ and C are mainly determined by empirical values so that the optimal recognition precision is difficult to realize. To improve the extraction accuracy of SVM, optimized strategies should be explored. Owing to the overwhelming advantages, PSO, GA

and FA algorithms have been widely used to optimize the performance of the recognition algorithms in many fields [23]–[25]. Based on this, the mentioned three algorithms are utilized to optimize C and σ of the non-linear SVM in BOTDA. The principles of the three optimization algorithms are explained subsequently.

2.2.1 PSO-SVM: PSO is an optimization algorithm based on iterative pattern and it is designed by simulating the predator behavior of birds. The algorithm is initially a group of random particles, and then finds the best solution through continuous iteration. The number of particles is set to be N, which is $X = (X_1, X_2, \ldots, X_i, \ldots, X_N)$. Each particle has two parameters of speed $V_i = (v_{i1}, v_{i2}, \ldots, v_{id}, \ldots, v_{iD})$ and position $X_i = (x_{i1}, x_{i2}, \ldots, x_{id}, \ldots, x_{iD})$ in the D-dimensional space, which represent the speed and direction of movement, respectively. In each iteration, the particle updates itself by looking for two extreme values (P_i and P_g), the first one is the optimal solution $P_i = (p_{i1}, p_{i2}, \ldots, p_{id}, \ldots, p_{iD})$ which is found by the particle itself and the second one is the global optimal solution $P_g = (p_{g1}, p_{g2}, \ldots, p_{gd}, \ldots, p_{gD})$ found by the entire population. V and X of each particle are updated according to the following expressions until the two optimal solutions are found.

$$v_{id}^{t+1} = w v_{id}^{t} + c_1 rand_1(p_{id}^{t} - x_{id}^{t}) + c_2 rand_2(p_{gd}^{t} - x_{id}^{t}) \tag{5}$$

$$x_{id}^{t+1} = x_{id}^{t} + v_{id}^{t+1} \tag{6}$$

where w is inertia weight and it determines the optimization ability, c_1 and c_2 are the acceleration constants, *rand()* is a random equation and t is the sequence number of iteration, x_{id}^{t} represents the current value of the SVM parameters C and σ, v_{id} determines the direction and size in the next update. Till the preset conditions are satisfied, the iteration is completed and the optimal C and σ are obtained.

Generally, the parameters in PSO (including maximum number of iterations, population size, w, c_1 and c_2) are determined empirically [28]. To acquire the appropriate values, we firstly iterate these variables through. According to the results, the maximum number of iterations and the number of population are assigned as 100 and 200, respectively. c_1, c_2 and w are 1.7, 1.5 and 1, respectively.

2.2.2 GA-SVM: GA is an optimized algorithm based on the evolution theory and genetics. Through calculating the fitness of each chromosome, the optimal one in an encoded parameter space can be targeted by using randomization techniques. Finally, the best chromosome is chosen to represent the best solution. The flow chart of GA algorithm is depicted in Fig. 2. Firstly, a set of SVM parameters of C and σ are randomly generated and encoded. Then we initialize the population and calculate the fitness of them. The fitness decreases with the increase of the SVM error. If the fitness is larger than the threshold value, the optimal parameters are obtained by comparison. Otherwise the population should be processed with selection, cross and mutation methods. After that, the next progeny population is generated and its fitness is calculated again until it exceeds the threshold value. Especially, the selection is implemented with the roulette wheel and it is expressed by

$$P_i = F_i / \sum_{j=1}^{n} F_j \tag{7}$$

where F_i is the fitness of individuals, n is the number of individuals in a population.

Similar to PSO algorithm, the appropriate parameters of GA are obtained through traversing [29]. The maximum number of iterations and the size of population are 100 and 200, respectively. The cross rate and the mutation rate are fixed at 0.7 and 0.2, respectively.

2.2.3 FA-SVM: FA is based on the luminescence characteristics of the firefly and it realizes random optimization. A feasible solution is simulated as a firefly. The location and brightness of the firefly correspond to the optimization object and target, respectively. Each firefly attracted by a brighter firefly corresponds to the optimization process, then it continuously gathers towards the brightest one till the end. The brightest firefly denotes the optimal combination of C and σ in SVM.

The degree of mutual attraction between the two fireflies is related to two parameters. One is the brightness of the firefly (I), the other is the distance between two fireflies (T). The brightness is

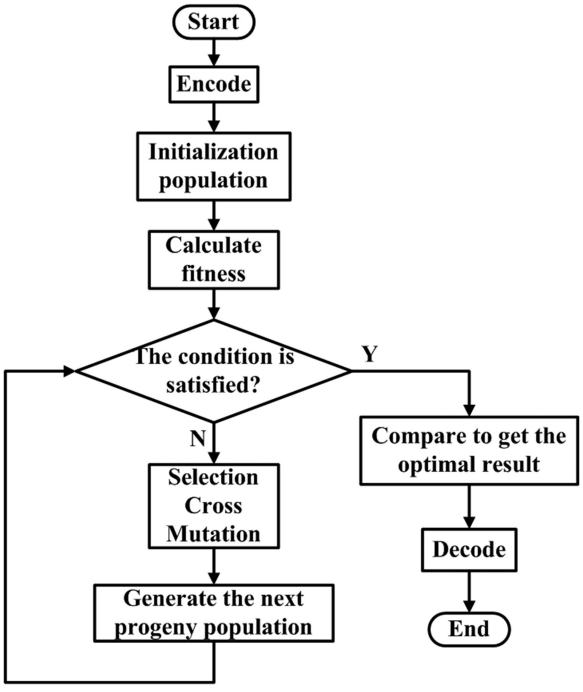

Fig. 2. The flow chart of GA algorithm.

related to distance and propagation medium so that the relative fluorescence brightness of firefly *i* to firefly *j* can be described as

$$I(T_{ij}) = I_i e^{-\gamma T_{ij}^2} \tag{8}$$

where I_i is the brightness of the brightest firefly and is related to the value of the objective function. Higher brightness can be obtained with the optimization of the function parameters. γ is the optical absorption coefficient and it is usually set as a constant. T_{ij} is the distance between firefly *i* and *j*. Since I_{ij} is proportional to the attraction between firefly *i* and firefly *j*, the mutual attraction between the two fireflies can be expressed by

$$\beta(T_{ij}) = \beta_0 e^{-\gamma T_{ij}^2} \tag{9}$$

where β_0 represents the maximum degree of attraction. According to the attraction between two fireflies, the firefly *j* moves toward to *i* and its position is updated simultaneously. The position of firefly *j* is updated according to the following expression

$$x_j^{t+1} = x_j^t + \beta(T_{ij})(x_i^t - x_j^t) + \alpha(rand - 1/2) \tag{10}$$

where x_i and x_j represent the position of firefly *i* and *j*, α is step factor, *rand* is a random factor with uniform distribution and it is limited in the range of [0,1]. *t* is the sequence number of iteration. Similar to another two methods [30], the maximum number of iterations and the number of fireflies are 100 and 200, respectively. The step factor α is fixed at 0.5 and β_0 is 0.2.

2.3 Algorithm Phases of Optimized SVM

Fig. 3 depicts the training and testing phases of the optimized-SVM algorithm to obtain the temperature information. According to the theoretical analysis and property of the actual BGS, where the actual BGS has a line shape between Lorentzian curve and Gaussian Curve, it can be approximated by pseudo-Voigt curves. Thus, the pseudo-Voigt curves are acted as the training

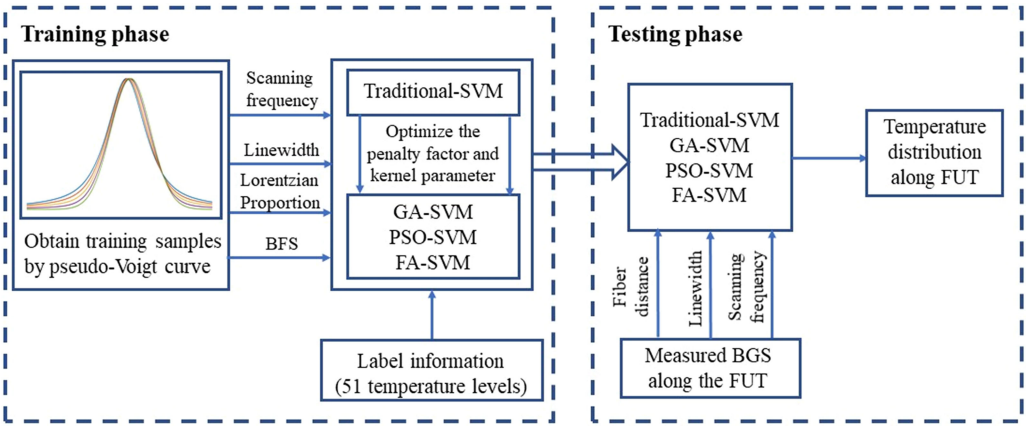

Fig. 3. Training and testing phases of the optimized-SVM algorithms for accurate temperature extraction in BOTDA.

samples. After processing by the optimized SVM algorithms, the input curves are converted into different temperature scales in the training phase.

To verify the robustness of the optimized-SVM algorithms, the parameters of fiber distance, BGS linewidth and scanning frequency step are changed in experiment, as illustrated in testing phase of Fig. 3. In experiment, the measured BGS along the fiber under test (FUT) is used as the inputs of the optimized algorithms to extract the temperature information.

2.4 Simulation Results and Discussions

In the simulation process, pseudo-Voigt curve is used as the ideal actual BGS curve and it is a combination of Lorentz and Gaussian curves [10]:

$$f(v) = g_B \left\{ c \frac{1}{1 + [(v - v_B)/(\Delta v_B/2)]^2} + (1 - c) \exp\left[-\ln 2 \left(\frac{v - v_B}{\Delta v_B/2} \right)^2 \right] \right\} \tag{11}$$

where g_B is the peak gain, v_B is the BFS, Δv_B is the linewidth of the BGS, v is frequency, c is the proportion of the Lorentzian component. For the temperature from 20 °C to 70 °C, 51-temperature scales are formed with step of 1 °C. Meanwhile, the temperature coefficient of 1.16209 MHz/°C is adopted to determine the BFS in the simulation. Here, the coefficient is calibrated with the FUT used in our experiment. The ideal BGS at each temperature scale is constructed according to pseudo-Voigt curves. The scanning frequency varies from 10.560 GHz to 10.760 GHz with step of 1 MHz. The linewidth of BGS ranges from 30 MHz to 100 MHz with step of 5 MHz. At the same time, the linear factor c ranges from 0 to 1 with step of 0.2. Thus, we can obtain $51 \times 15 \times 6$ training samples for SVM training.

To evaluate the performance of three optimized SVM algorithms for extracting temperature information from BGS, the effect of SNR on the BFS extraction is firstly verified. In the simulations, the BGS linewidth and the scanning step are fixed at 50 MHz and 1 MHz, respectively. Theoretically, the BGS linewidth corresponds to 20 ns pump pulse. Meanwhile, Gaussian white noise is added into the BGS curves to tune the SNR from 2 dB to 14 dB. Here, the SNR is defined as the ratio between the mean of the peak value (V_{peak}) at the peak frequency trace and its standard deviation (δ_N), $SNR = 10 * log10(V_{peak}/\delta_N)$ [20]. For ensuring the reliability of the result, 1000-times average has been performed to process the demodulation results in the simulation process. Note that, the traditional SVM algorithm has also been implemented to act as the reference. After processing with PSO-SVM, GA-SVM, FA-SVM and traditional SVM algorithms for the BGS curves, both of the root mean square error (RMSE) and the coefficient of determination (R^2) are calculated at different

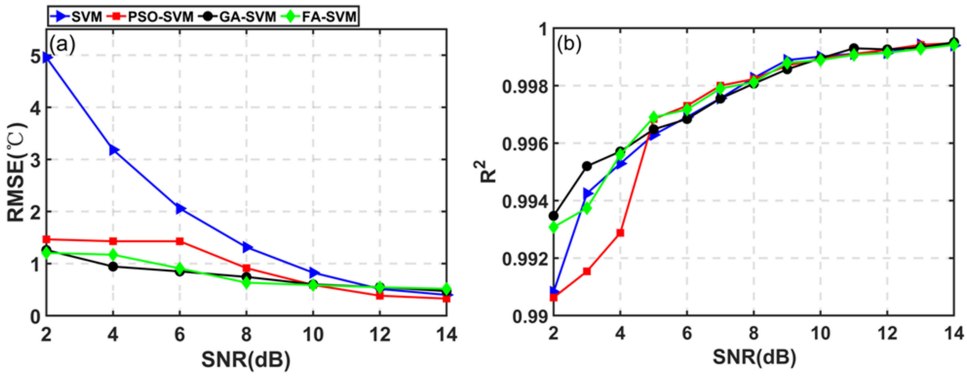

Fig. 4. (a) RMSE (the temperature is set at 60 °C) and (b) R^2, computing under different SNR.

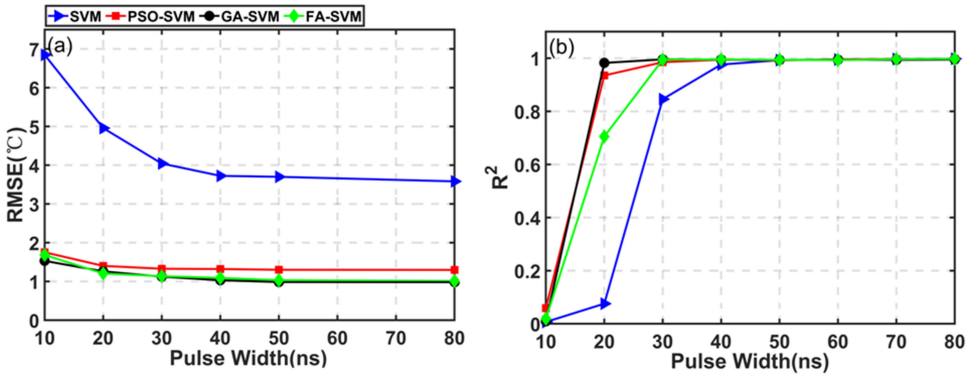

Fig. 5. (a) RMSE (the temperature is set at 60 °C) and (b) R^2, computing at different pump pulse widths.

SNRs, as illustrated in Fig. 4. Here, the RMSE is calculated using the demodulated temperatures extracting by four different SVM algorithms, where the target temperature is set at 60 °C. The R^2 represents the degree of fitting for all temperature scales predictions and its maximum value is 1 (i.e., the closer to 1 means the better fitting result). As depicted in Fig. 4(a), the RMSE reduces with the decrease of SNR for all algorithms. That means the demodulation accuracy increases with the SNR increase of BGSs. Compared with the traditional SVM, higher demodulation accuracy (i.e., smaller RMSE values) can be obtained for the optimized algorithms (PSO-SVM, GA-SVM and FA-SVM), especially for the SNR less than 11 dB. For the optimized algorithms, GA-SVM and FA-SVM algorithms have equal performance, while the PSO-SVM algorithm is slightly worse than them at low SNR. Conversely, PSO-SVM algorithm achieves best accuracy in the four algorithms when the SNR exceeds 10 dB. In terms of R^2, the optimized algorithms have approximate performance in comparison with the traditional SVM. Among them, GA-SVM is slightly better than the other algorithms. In conclusion, the modification SVM algorithms have better performance than the traditional SVM, especially for the low SNR.

In addition to the SNR, the linewidth of BGS also has huge effect on the extraction performance of the SVM. Due to the BGS linewidth is mainly determined by the pulse width of the pump, so the effect of the BGS linewidth is converted into the effect of the pulse width on the demodulation performance of SVM. In the simulation, the SNR of the BGS curves and the scanning step are set to 2 dB and 1 MHz, respectively. Meanwhile, the pump pulse width ranges from 10 ns to 80 ns. The simulated results are shown in Fig. 5 and the optimized SVM algorithms improve the extraction accuracy greatly (i.e., the smaller RMSE) in comparison with the traditional SVM. In the simulations,

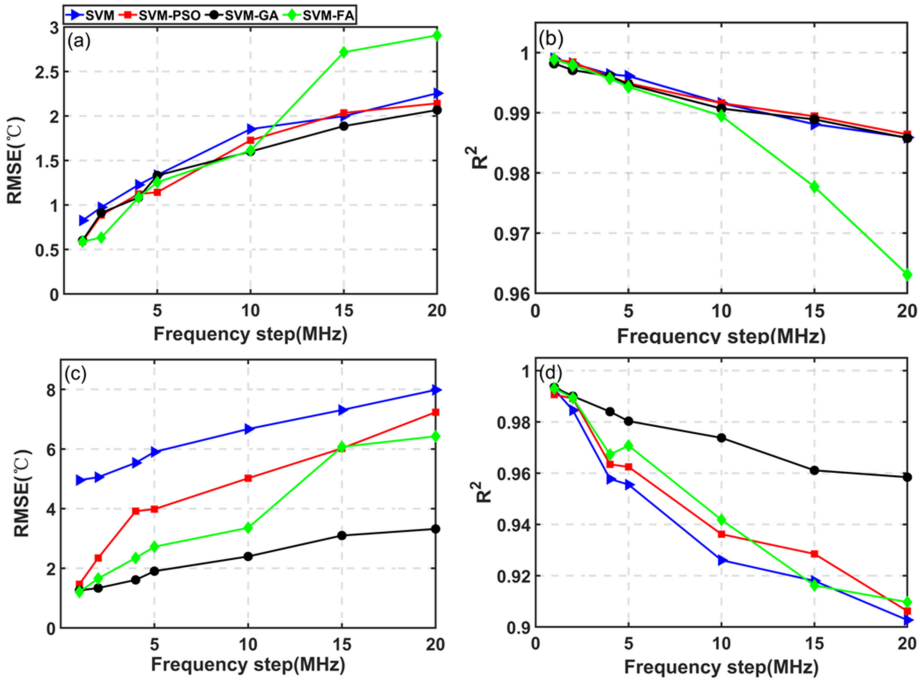

Fig. 6. (a) RMSE (the temperature is set at 60 °C) at SNR of 10 dB, (b) R^2 at SNR of 10 dB, (c) RMSE (the temperature is set at 60 °C) at SNR of 2 dB, (d) R^2 at SNR of 2 dB, computing under different frequency scanning steps.

the RMSE improvement over 3 °C and the maximum improvement exceeds 5 °C at the narrow pump pulse width. For the R^2, as illustrated in Fig. 5(b), the three optimized SVM algorithms have significant improvements when the pump pulse is less than 40 ns. According to the above analysis, we can find that both of the RMSE and R^2 have been improved greatly by adopting the optimized SVM algorithms. Besides, the result shows great tolerance for changes of pump pulse width.

Except for the SNR and BGS bandwidth, the demodulation of the SVM algorithm also varies with the change of the scanning step. The number of feature points in each BGS is determined by the scanning step size. That greatly affects the accuracy of temperature extraction. Thus, the performance variation of three optimization algorithms induced by the changing step size should also be discussed. The linewidth of BGS is fixed at 50 MHz during simulation. Meanwhile, two different SNRs of 10 dB and 2 dB have been verified and the results are shown in Fig. 6. With the increase of the frequency scanning step, the feature points on each BGS reduce so that the RMSE increase and the R^2 reduce gradually. When a high SNR of 10 dB is adopted, as depicted in Fig. 6(a) and 6(b), there is no significant difference in temperature extraction for all algorithms. However, both of the RMSE and R^2 are obviously enhanced when a low SNR of 2 dB is selected, as shown in Fig. 6(c) and 6(d). It must be noted that the GA-SVM algorithm shows the best performance improvements in both high and low SNR. In other words, at low SNR, the optimized SVM algorithm has higher robustness at the large frequency steps than traditional SVM algorithm. That can reduce the processing time significantly.

3. Experiment Results and Verification

3.1 Experimental Platform

The BOTDA experimental setup for collecting data is depicted in Fig. 7. A distributed feedback laser (DFB) with peak power of 10 dBm and center wavelength of 1549 nm is used as the light source. The continuous wave (CW) light is split into two branches by a 50:50 coupler. The upper

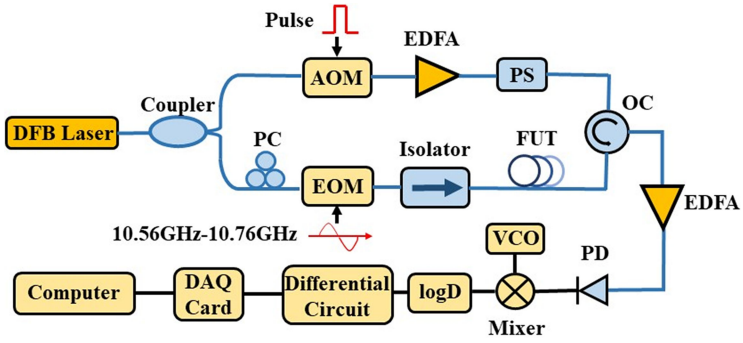

Fig. 7. The experiment setup of BOTDA system.

branch is pulsed by an acousto-optic modulator (AOM) with an extinction ratio of 50 dB. Then the peak power of the pump light is amplified to 18 dBm by an erbium doped fiber amplifier (EDFA). After passing through a polarization scrambler (PS) which is used to eliminate polarization noise, the pump pulse enters the FUT via an optical circulator (OC). The lower branch of light beam is modulated by the microwave signal generating with an electro-optical modulator (EOM). Here, the frequency of the microwave signal tunes from 10.560 GHz to 10.760 GHz. At the output of the EOM, an isolator is connected to resist the return light. In the sensing fiber, two beams lights generate stimulated Brillouin amplification effect and the scattered light is converted into an electrical signal at the photo-detector (PD). After that, the electrical signal (10.56 GHz-10.76 GHz) is converted into the intermediate frequency (IF) signal (760MHz-960MHz) through mixing with the local electrical signal (with frequency of 9.8 GHz) at an electrical mixer. The local electrical signal is generated by a voltage-controlled oscillator (VCO). After converting the IF signals into the BGS traces, they are collected by a data acquisition card (DAQ) with 100 MS/s sample rate and 12-bits precision. Finally, the BGS traces are processed with a personal computer.

3.2 Experiment Results

Before the training process, we calculate the relationship between BFS and temperature based on the built BOTDA platform. In the test, a 50-m test fiber is heated with a temperature controller and the applied temperature increases from 10 °C to 60 °C with step of 1 °C. The scanning frequency of the microwave source ranges from 10.560 GHz to 10.760 GHz with step of 1 MHz. To ensure the reliability of the relationship, 1000-times average is performed at each scanning point. In experiment, we reduce the SNR through tuning the gain of EDFA (before PD) to prove the advantage of the optimized algorithms in low SNR. To avoid the polarization noise, the reduction of the averaging times is not adopted here. At last, the BFS is extracted with pseudo-Voigt curve fitting method within the 50-m test fiber. The relationship between temperature T and BFS υ_B is fitted as:

$$\upsilon_B = 1.16209 \times 10^{-3} T + 10.6437 \tag{12}$$

In the experiment, a 40-km single mode fiber (SMF) is adopted as the FUT in the testing phases. 40-ns pump pulse and different scanning steps of 1 MHz, 2 MHz, 5 MHz, 10 MHz, 15 MHz and 20 MHz have been used. Here, 1000-times average is performed to improve the SNR. While in the testing phase each measured BGS as the testing sample is classified into one class of temperature, i.e., Class1, Class2…Class51, by the traditional SVM and three optimized SVM, respectively. Thereby the corresponding temperature value is set as the measured temperature. Fig. 8 shows the collected 3D BGSs (obtaining at 1-MHz scanning step), they are put into the trained SVM model to verify the simulation results in Section 2. At the end of the fiber, 50-m fiber section is heated to 60 °C. Fig. 9(a) shows the temperature distribution along the 40-km fiber. To

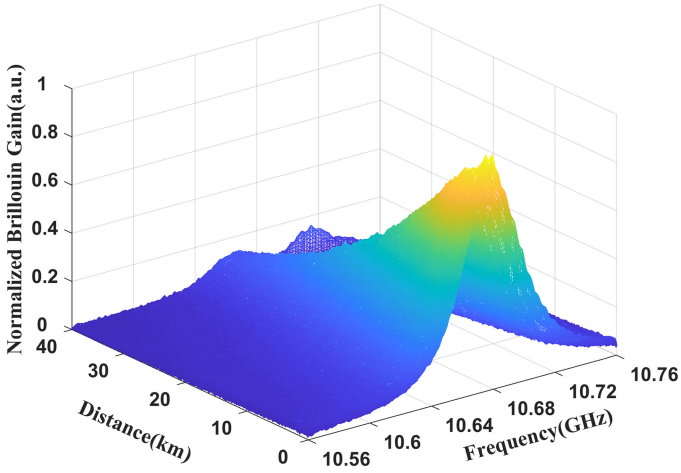

Fig. 8. The measured BGS distribution along 40 km FUT with 1 MHz frequency scanning step.

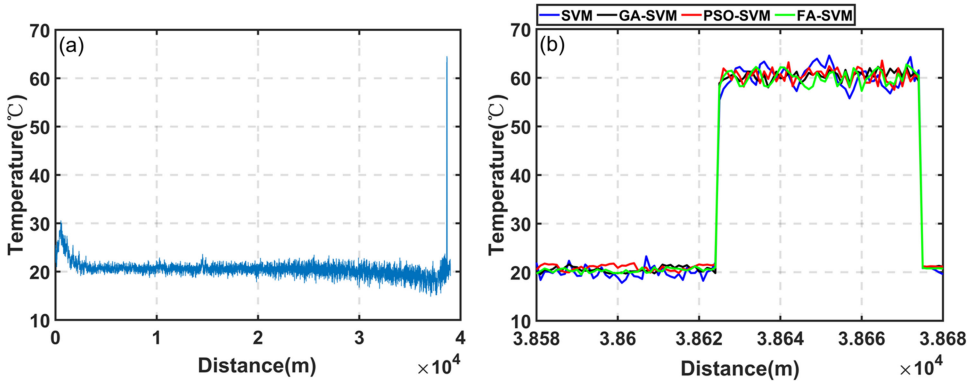

Fig. 9. (a) The temperature extraction distribution along 40 km FUT extracted by traditional SVM. (b) The zoom-in view of temperature distribution at the heated section extracted by four different algorithms.

clearly observe the hotspot, the temperature distribution of 50-m fiber is illustrated in Fig. 9(b). Compared to the results processing with the traditional SVM algorithm (the blue line), the results processing with the optimized algorithms are more smooth (small jitter), especially for the GA-SVM algorithm (the black line). Meanwhile, the standard deviations (at the hotspot) processing with four methods are calculated and they are 4.3271 °C, 1.2601 °C, 1.3574 °C and 1.7624 °C for SVM, GA-SVM, FA-SVM and PSO-SVM algorithms, respectively. It can be seen that GA-SVM achieves best performance among these algorithms at a low SNR(∼2.5 dB). Compared with the traditional SVM, the measurement accuracy improves about 5.4 dB.

The BGSs collected at different distances are used to verify the impact of the SNR on the demodulation results. In this test, the pump pulse and the frequency scanning step are fixed at 40 ns and 1 MHz. The BGSs at the position of 5 km, 10 km, 15 km, 20 km, 25 km, 30 km, 35 km, 40 km are used as the validation data. Due to the inherent loss, the SNR decreases with the fiber length. The SNR at the head end and tailing end are 10.5 dB and 2.5 dB, respectively. The traditional SVM algorithm and three optimized SVM algorithms are used to extract the temperature from the BGSs at different locations (different SNRs). Fig. 9 depicts the demodulation results and the experimental results are in consistent with the simulations. As shown in Fig. 10(a), three optimized-SVM algorithms improve the accuracy greatly in comparison with traditional SVM (the

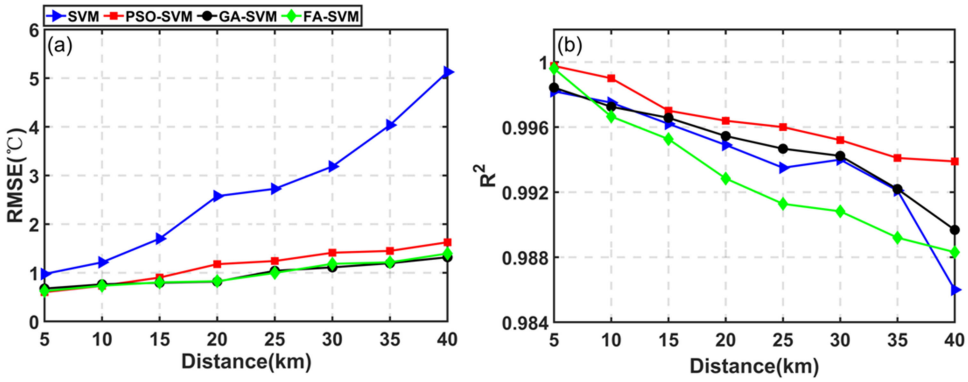

Fig. 10. (a) RMSE (the measured temperature is 60 °C) and (b) R^2, calculating from the experimental BGSs under different fiber distances.

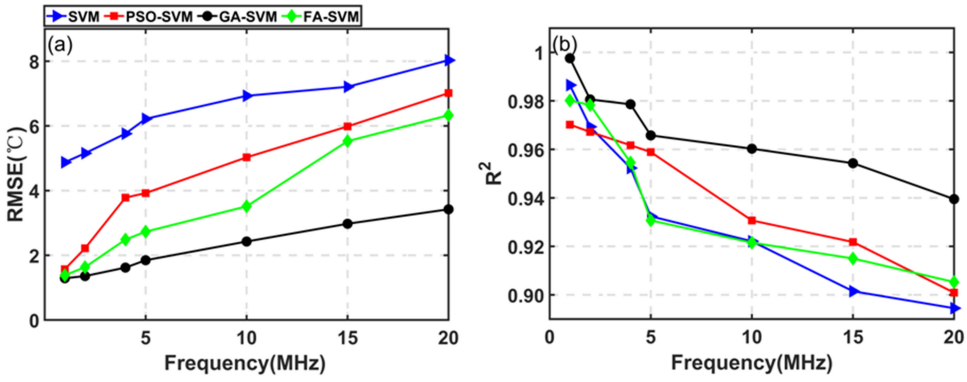

Fig. 11. (a) RMSE (the measured temperature is 60 °C) and (b) R^2, based on measured BGSs under different frequency scanning steps.

blue line). Fig. 10(b) presents the degree of fitting and the optimized algorithms has approximate R^2 as the traditional SVM.

Besides, the frequency scanning step has a great impact on the temperature extraction accuracy. Hence, we further discuss the performance of three optimization models by tunning the frequency scanning step. The same frequency scanning steps as the simulation are performed in the experiment. The width of the pump pulse and the SNR are 40-ns and ∼2.5 dB, respectively. The verification results are illustrated in Fig. 11. With the increase of the frequency scanning step, as illustrated in Fig. 11(a), the RMSE grows for all algorithms. Compared with the traditional SVM algorithm, the optimized SVM algorithms improve the extraction accuracy greatly and the maximum enhancement of 4 °C is achieved by GA-SVM. Fig. 11(b) shows the degree of fitting R^2, it decreases with the step increase. Similarly, the optimized algorithms have significant enhancement in comparison with the traditional SVM.

It should be mentioned that the processing time of temperature extraction from BGSs is also an important factor to evaluate the performance of these algorithms. Here, the processing time refers to online testing time. Considering the real-time nature of the training process, the training time is also listed as a reference the comparison of the processing time and the training time are listed in Table 1. All of results are measured by using Matlab with i7-8750H CPU and 32G RAMs. Compared to the LCF (tens of minutes), the processing time using three optimized SVM algorithms to extract temperature in the testing phase are only 14.68 seconds (tens of seconds). Although the optimized

TABLE 1
Comparison of Processing Time of Temperature Extraction Along 40 km Fiber

Frequency Step	SVM(s)		PSO-SVM(s)		GA-SVM(s)		FA-SVM(s)		LCF(s)
	Training	Testing	Training	Testing	Training	Testing	Training	Testing	
1 MHz	1.09	14.72	76.64	14.68	86.95	14.25	54.08	14.43	1830.6
2 MHz	1.02	10.26	52.51	10.02	57.94	10.21	24.27	10.24	1351.2
4 MHz	0.68	9.34	49.61	10.11	51.13	10.15	21.97	10.22	1302.0
5 MHz	0.52	9.22	42.39	9.89	44.59	10.02	18.60	9.89	1279.2
10 MHz	0.31	8.01	36.88	9.92	40.21	9.95	13.70	9.94	1233.6

TABLE 2
Comparison Between the Proposed Optimized SVM and GS Based SVM (10-dB SNR and 1-MHz Frequency Step)

Algorithms	Stride	C	δ	RMSE	Std	Time (s)	
						Training	Testing
GA-SVM	—	3.509	0.027	1.481	0.056	45.97	10.21
GS-SVM	s_c=0.1,	3.4	0.1	1.578	0.101	265.22	10.46
FA-SVM	—	2.963	0.024	2.164	0.105	21.29	10.23
GS-SVM	s_c=1, s_σ=0.1	4	0.4	2.677	0.147	22.53	10.14
PSO-SVM	—	5.650	0.514	3.514	0.112	42.31	10.35
GS-SVM	s_c=1, s_σ=0.5	16	1	3.742	0.195	4.21	9.98

TABLE 3
Comparison Between the Proposed Optimized SVM and GS Based SVM (4-dB SNR and 4-MHz Frequency Step)

Algorithms	Stride	C	δ	RMSE	Std	Time (s)	
						Training	Testing
GA-SVM	—	3.509	0.027	1.481	0.056	45.97	10.21
GS-SVM	s_c=0.1,	3.4	0.1	1.578	0.101	265.22	10.46
FA-SVM	—	2.963	0.024	2.164	0.105	21.29	10.23
GS-SVM	s_c=1, s_σ=0.1	4	0.4	2.677	0.147	22.53	10.14
PSO-SVM	—	5.650	0.514	3.514	0.112	42.31	10.35
GS-SVM	s_c=1, s_σ=0.5	16	1	3.742	0.195	4.21	9.98

algorithms take slightly more time than the traditional SVM in the training time, even if the SVM training time is included in the data processing time, the processing speed using three optimized algorithms are still 20-fold faster than that using LCF. So, it is acceptable by considering the great improvement of the extraction accuracy.

Grid search (GS) is a commonly used method to realize the optimization of algorithms just containing one variable. In non-linear SVM, two variables/parameters need to be optimized so that we choose the proposed algorithms. To validate the advantages of the used algorithms, the comparison between the utilized optimized algorithm and the common grid search (GS) is performed. The comparison results are listed in Table 2. In this comparison, RMSE and time are used to evaluate the performances of these algorithms. Here, the SNR and frequency step are 10 dB and 1 MHz, respectively. In this table, stride represents the tuning step, C and δ are the key parameters in non-linear SVM. It can be seen that the achieved RMSE reduces when smaller steps are adopted. However, the training time increases sharply. Compared to GS-SVM, the utilized algorithms take less time when same RMSE is acquired. That indicates the proposed algorithms are better than the simple GS-SVM. To validate the advantages of the proposed algorithms over the GS based SVM completely, 4-dB SNR and 4-MHz frequency step are also employed. As illustrated in Table 3, the GS based SVM takes much longer time to obtain the same RMSE.

4. Conclusion

In this work, we propose and demonstrate three optimized SVM algorithms to improve the demodulation accuracy in SVM based BOTDA. Both in the simulation and experiment, the impact of the different conditions on the demodulation accuracy have been verified. The extraction accuracy for the temperature by adopting three optimized algorithms is improved significantly compared to the traditional SVM algorithm. In the experiment, about 4-°C accuracy improvement is achieved at the end of the fiber (40-km, ∼2.5-dB SNR) by using 1-MHz scanning step and 40-ns pump pulse. That is in good consistent with the simulation. It should be noted that the better enhancement can be realized by adopting larger scanning step.

Among the optimized algorithms, the PSO-SVM algorithm has the best optimized performance if the sensing system possesses high SNR (over 10 dB), the GA-SVM algorithm has the best optimization performance when the SNR is smaller than 10 dB, while the FA-SVM algorithm owns the fastest processing speed. Although more processing time is required in comparison with the conventional SVM, the optimized SVM algorithms illustrate high significance for the accurate temperature extraction. Besides, the processing speed is faster than the curve fitting method over 20-times. Hence the optimized SVM algorithms are the alternative methods to promote the measurement accuracy and response speed of BOTDA sensor systems.

References

[1] G. Y. Yang, X. Y. Fan, S. Wang, B. Wang, Q. W. Liu, and Z. Y. He, "Long-range distributed vibration sensing based on phase extraction from phase-sensitive OTDR," *IEEE Photon. J.*, vol. 8, no. 3, Jun. 2016, Art. no. 6802412.

[2] C. A. Galindez-Jamioy and J. M. Lopez-Higuera, "Brillouin distributed fiber sensors: An overview and applications," *J. Sensors*, vol. 2012, 2012, Art. no. 204121.

[3] X. H. Zou *et al.*, "Microwave photonics for featured applications in high speed railways: Communications, detection, and sensing," *J. Lightw. Technol.*, vol. 36, no. 19, pp. 4337–4346, Oct. 1, 2018.

[4] W. L. Zhang *et al.*, "Random distributed feedback fiber laser based on combination of Er-doped fiber and single-mode fiber," *IEEE J. Sel. Topics Quantum Electron.*, vol. 21, no. 1, pp. 44–49, Jan./Feb. 2015.

[5] H. Q. Chang *et al.*, "DBA-based BOTDA using optical comb pump and pulse coding with a single laser," *IEEE Photon. Technol. Lett.*, vol. 28, no. 10, pp. 1142–1145, May 15, 2016.

[6] M. Chen, Z. Meng, J. F. Wang, and W. Chen, "Strong linewidth reduction by compact Brillouin/erbium fiber laser," *IEEE Photon. J.*, vol. 6, no. 5, Oct. 2014, Art. no. 1502107.

[7] M. Chen, Z. Meng, Y. C. Zhang, J. F. Wang, and W. Chen, "Ultranarrow-linewidth Brillouin/erbium fiber laser based on 45-cm erbium-doped fiber," *IEEE Photon. J.*, vol. 7, no. 1, Feb. 2015, Art. no. 1500606.

[8] C. Li and Y. Li, "Fitting of Brillouin spectrum based on LabVIEW," in *Proc. 5th Int. Conf. Wireless Commun., Netw., Mobile Comput.*, 2009, pp. 1–4.

[9] J. Dhliwayo, D. J. Webb, and C. N. Pannell, "Statistical analysis of temperature measurement errors in a Brillouin scattering-based distributed temperature sensor," *Proc. SPIE*, vol. 2838, pp. 276–286, 1996.

[10] C. Zhang, Y. Yang, and A. Li, "Application of Levenberg–Marquardt algorithm in the Brillouin spectrum fitting," *Proc. SPIE*, vol. 7129, 2008, Art. no. 71291Y.

[11] W. Zou, Z. He, and K. Hotate, "Complete discrimination of strain and temperature using Brillouin frequency shift and birefringence in a polarization-maintaining fiber," *Opt. Express*, vol. 17, no. 3, pp. 1248–1255, 2009.

[12] X. Bao, A. Brown, M. Demerchant, and J. Smith, "Characterization of the Brillouin-loss spectrum of single mode fibers by use of very short (<10-ns) pulses," *Opt. Lett.*, vol. 24, no. 8, pp. 510–512, 1999.

[13] G. A. Ferrier, S. Afshar, X. Bao, and L. Chen, "A new fitting method for spectral characterization of Brillouin based distributed sensors," *Appl. Photon. Technol.*, vol. 5260, pp. 512–515, 2003.

[14] M. A. Farahani, E. Castilloguerra, and B. G. Colpitts, "Accurate estimation of Brillouin frequency shift in Brillouin optical time domain analysis sensors using cross correlation," *Opt. Lett.*, vol. 36, no. 21, pp. 4275–4277, 2011.

[15] A. K. Azad, L. Wang, N. Guo, C. Lu, and H. Y. Tam, "Temperature sensing in BOTDA system by using artificial neural network," *Electron. Lett.*, vol. 20, no. 51, pp. 1578–1580, 2015.

[16] A. K. Azad, L. Wang, N. Guo, H. Y. Tam, and C. Lu, "Signal processing using artificial neural network for BOTDA sensor system," *Opt. Express*, vol. 24, no. 6, pp. 6769–6782, 2016.

[17] C. W. Hsu and C. J. Lin, "A comparison of methods for multiclass support vector machines," *IEEE Trans. Neural Networks*, vol. 13, no. 2, pp. 415–425, Mar. 2002.

[18] C. Cortes and V. Vapnik, "Support-vector networks," *Mach. Learn.*, vol. 20, no. 3, pp. 273–297, 1995.

[19] L. Bottou and C. J. Lin, "Support vector machine solvers," in *Large Scale Kernel Machines*. Cambridge, MA, USA: MIT Press, vol. 3, no. 1, pp. 301–320, 2007.

[20] H. Wu, L. Wang, N. Guo, C. Shu, and C. Lu, "Brillouin optical time domain analyzer assisted by support vector machine for ultrafast temperature extraction," *J. Lightw. Technol.*, vol. 35, no. 19, pp. 4159–4167, Oct. 1, 2017.

[21] H. Wu, L. Wang, N. Guo, C. Shu, and C. Lu, "Support vector machine assisted BOTDA utilizing combined Brillouin gain and phase information for enhanced sensing accuracy," *Opt. Express*, vol. 25, no. 25, pp. 31210–31220, 2017.

[22] H. Wu, L. Wang, N. Guo, C. Shu, and C. Lu, "Support vector machine based differential pulse-width pair Brillouin optical time domain," *IEEE Photon. J.* vol. 10, no. 4, Aug. 2018, Art. no. 6802911.
[23] S. W. Lin, K. C. Ying, S. C. Chen, and Z. L. Lee, "Particle swarm optimization for parameter determination and feature selection of support vector machines," *Expert Syst. Appl.*, vol. 35, no. 4, pp. 1817–1824, 2008.
[24] C. L. Huang and C. J. Wang, "A GA-based feature selection and parameters optimization for support vector machines," *Expert Syst. Appl.*, vol. 31, no. 2, pp. 231–240, 2006.
[25] A. U. Haque, M. H. Nehrir, and P. Mandal,"A hybrid intelligent model for deterministic and quantile regression approach for probabilistic wind power forecasting," *IEEE Trans. Power Syst.*, vol. 29, no. 4, pp. 1663–1672, Jul. 2014.
[26] C. W. Hsu, C. C. Chang, and C. J. Lin, "A practical guide to support vector classification," Nat. Taiwan Univ., Taipei, Taiwan, Tech. Rep., 2003. [Online]. Available: https://www.researchgate.net/publication/2926909_A_Practical_Guide_to_Support_Vector_Classification_Chih-Wei_Hsu_Chih-Chung_Chang_and_Chih-Jen_Lin
[27] V. Cherkassky and Y. Q. Ma, "Practical selection of SVM parameters and noise estimation for SVM regression," *Neural Netw.*, vol. 17, no. 1, pp. 113–126, 2004.
[28] R. Eberhart and Y. Shi, "Particle swarm optimization: Developments applications and resources," in *Proc. IEEE Congr. Evol. Comput.*, 2001, vol. 1, pp. 81–86.
[29] J. D. Schaffer, "A study of control parameters affecting online performance of genetic algorithms for function optimization," in *Proc. 3rd Int. Conf. Genetic Algorithms*, 1989, pp. 51–60.
[30] X. S. Yang, "Firefly algorithm, stochastic test functions and design optimisation," *Int. J. Bio-inspired Comput.*, vol. 2, no. 2, pp. 78–84, 2010.